nature ecology & evolution

ARTICLES

https://doi.org/10.1038/s41559-018-0722-0

Evolution and extinction of the giant rhinoceros *Elasmotherium sibiricum* sheds light on late Quaternary megafaunal extinctions

Pavel Kosintsev[1], Kieren J. Mitchell[2], Thibaut Devièse[3], Johannes van der Plicht[4,5], Margot Kuitems[4,5], Ekaterina Petrova[6], Alexei Tikhonov[6], Thomas Higham[3], Daniel Comeskey[3], Chris Turney[7,8], Alan Cooper[2], Thijs van Kolfschoten[5], Anthony J. Stuart[9] and Adrian M. Lister[10]*

Understanding extinction events requires an unbiased record of the chronology and ecology of victims and survivors. The rhinoceros *Elasmotherium sibiricum*, known as the 'Siberian unicorn', was believed to have gone extinct around 200,000 years ago—well before the late Quaternary megafaunal extinction event. However, no absolute dating, genetic analysis or quantitative ecological assessment of this species has been undertaken. Here, we show, by accelerator mass spectrometry radiocarbon dating of 23 individuals, including cross-validation by compound-specific analysis, that *E. sibiricum* survived in Eastern Europe and Central Asia until at least 39,000 years ago, corroborating a wave of megafaunal turnover before the Last Glacial Maximum in Eurasia, in addition to the better-known late-glacial event. Stable isotope data indicate a dry steppe niche for *E. sibiricum* and, together with morphology, a highly specialized diet that probably contributed to its extinction. We further demonstrate, with DNA sequencing data, a very deep phylogenetic split between the subfamilies Elasmotheriinae and Rhinocerotinae that includes all the living rhinoceroses, settling a debate based on fossil evidence and confirming that the two lineages had diverged by the Eocene. As the last surviving member of the Elasmotheriinae, the demise of the 'Siberian unicorn' marked the extinction of this subfamily.

The rhinoceros family (Rhinocerotidae) was formerly much more diverse than it is today, with some 250 named species[1], of which only 5 remain. During the Miocene, around 23–5 million years ago (Ma), rhinoceroses were a dominant part of the large mammal fauna in Africa, Eurasia and North America. Phylogenetic analysis of fossil species has resolved two main lineages: the Rhinocerotinae, which includes all living species and the recently extinct woolly rhinoceros (*Coelodonta antiquitatis*), and the extinct Elasmotheriinae[2]. Based on morphological diagnoses of early remains, the two subfamilies are thought to have diverged very early in rhinoceros evolution, by at latest 35 Ma[2,3]. The Elasmotheriinae subsequently gave rise to some 20 genera, of which only *Elasmotherium* survived the Miocene, with *E. sibiricum* its last surviving member, although some authors have separated *Elasmotherium* from other members of the group and place it within Rhinocerotinae[4,5]. A spectacular megafaunal species of Eurasia, at around 3.5 tonnes, *E. sibiricum* was the largest Quaternary rhinoceros. *E. sibiricum* was also remarkable in its anatomy: relatively slender limbs indicating adaptation for running, despite its mass[6]; absence of incisors and canines; and—uniquely among rhinoceroses—continuously growing cheek teeth with distinctive, highly convoluted enamel plates. The presence of a massive single horn in *Elasmotherium* has been inferred from the bony protuberance on the frontal bone of the skull, which implies a horn base much larger than in any other rhinoceros, living or extinct; hence, the informal name 'Siberian unicorn' (Fig. 1). The known geographical ranges of both *E. sibiricum* and related (in some cases possibly synonymous) *Elasmotherium* species were very limited, with most confirmed records from Kazakhstan, western and central Russia, Ukraine, Azerbaijan and Uzbekistan, as well as isolated finds (referred to *E. caucasicum*) from Mongolia and China[2,7,8] (Fig. 2). *E. sibiricum* was thought to have become extinct by 200,000 years ago (200 ka), although recent, unconfirmed reports suggested that it might have persisted into the late Pleistocene[7,9]. Its ecological niche has been a matter of speculation, from grazing on dry steppes to foraging for roots in damp riverine environments[7].

Results

Direct dating of unambiguously identified remains is an essential prerequisite for determining the extinction chronology of late Quaternary megafauna[10]. Of a total of 25 *E. sibiricum* bone samples analysed in the present study, 23 contained sufficient collagen for radiocarbon dating (Supplementary Table 1 and Fig. 3). All samples were first dated by accelerator mass spectrometry (AMS) either at the Groningen Centre for Isotope Research (CIO) in The Netherlands (laboratory code GrA) or the Oxford Radiocarbon Accelerator Unit (ORAU) in the United Kingdom (laboratory code OxA) using routine procedures (see Methods). All nine samples yielding

[1]Institute of Plant and Animal Ecology, Ural Branch of the Russian Academy of Sciences, Yekaterinburg, Russia. [2]Australian Centre for Ancient DNA, School of Biological Sciences, University of Adelaide, Adelaide, Australia. [3]Oxford Radiocarbon Accelerator Unit, University of Oxford, Oxford, UK. [4]Center for Isotope Research, Groningen University, Groningen, The Netherlands. [5]Faculty of Archaeology, Leiden University, Leiden, The Netherlands. [6]Zoological Institute, Russian Academy of Sciences, Saint Petersburg, Russia. [7]Palaeontology, Geobiology and Earth Archives Research Centre, School of Biological, Earth and Environmental Sciences, University of New South Wales, Sydney, Australia. [8]Climate Change Research Centre, School of Biological, Earth and Environmental Sciences, University of New South Wales, Sydney, Australia. [9]Department of Biosciences, Durham University, Durham, UK. [10]Department of Earth Sciences, Natural History Museum, London, UK. *e-mail: A.Lister@nhm.ac.uk

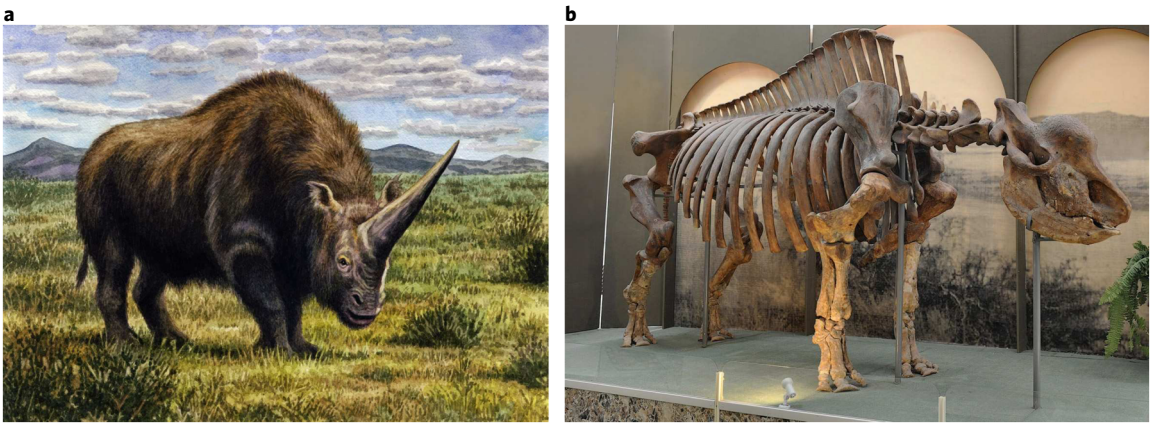

Fig. 1 | Artist's impression and mounted skeleton of *Elasmotherium* species. **a**, Artist's impression of *Elasmotherium*. **b**, Mounted skeleton of *E. sibiricum* from Gaevskaja Village near Stavropol, southwest Russia, on display in the Stavropol Museum (skeleton length: ~410 cm; height: 250 cm). Image credit: W. S. Van der Merwe (https://www.deviantart.com/willemsvdmerwe/); photo credit: Igor Doronin.

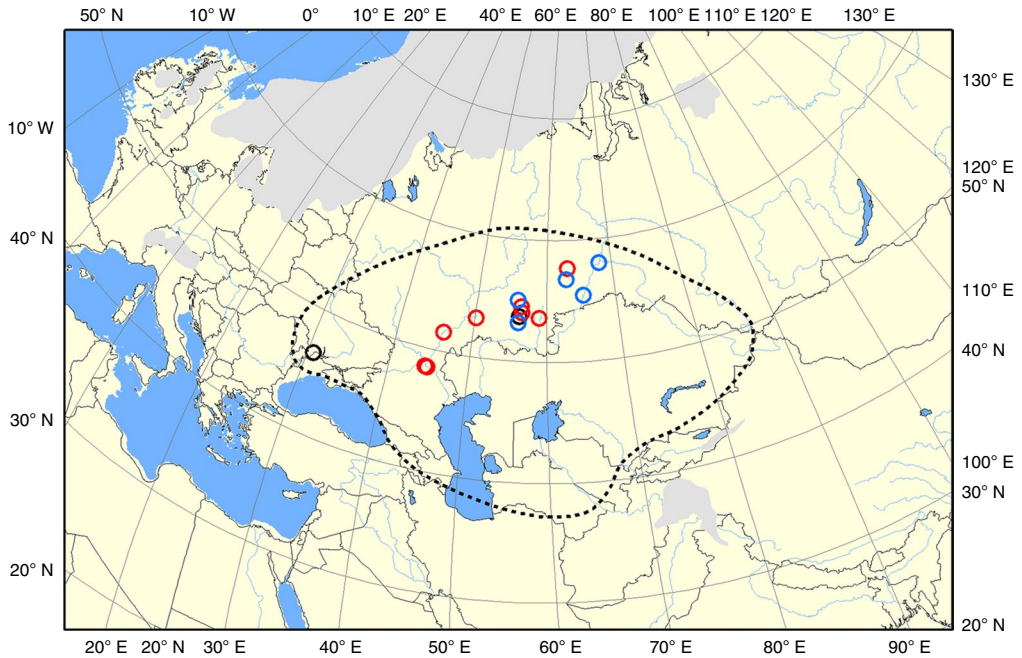

Fig. 2 | Map of distribution and samples analysed. The dashed line shows the total range of specimens referred to *E. sibiricum*[7,8]. Red circles represent samples producing radiocarbon and stable isotope data. Blue circles represent samples producing radiocarbon, stable isotope and DNA sequencing data. Black circles represent no collagen. Note that there are fewer mapped points than samples analysed because multiple samples were found at some localities. The map shows ice sheets (grey shading) and bathymetry for Marine Isotope Stage 3 (from refs [37,78,79]).

dates younger than 35,000 radiocarbon years were then cross-dated by the other laboratory (Supplementary Table 1), and the results were compared using a chi-squared test (Supplementary Table 8). In five of nine cases, the pairs of dates were not statistically distinguishable. However, for the other four paired samples, there was a discrepancy between the dates obtained in the two laboratories. In two cases, the dates obtained at the ORAU were older than those obtained at the CIO, and in the other two cases, the opposite was the case. These differences are probably due to contamination, which could not be totally removed using standard methods of collagen purification. For two samples (Institute of Plant and Animal Ecology (IPAE) 897/123 and Zoological Institute (ZIN) 36330), the difference between the dates obtained by the two laboratories was ~10,000 years. We therefore decided to undertake further dating of all nine samples using the single amino acid radiocarbon method developed at the ORAU[11]. This method involves the separation of the underivatized amino acids from hydrolysed bone collagen using preparative high performance liquid chromatography, isolating the amino acid hydroxyproline for AMS measurement. This pretreatment approach (coded 'HYP') is the most efficient available technique for removing contaminants, including (but not limited to) conservation materials (with the exception of collagen-based glue). All of the chronometric data from ORAU are reported in Supplementary Table 7. Chi-squared tests showed that in four of the cases, the dates obtained on ultrafiltered collagen and hydroxyproline were not statistically distinguishable (Supplementary Table 8), indicating that all the contaminant had been removed by the AF/AF* treatment (see Methods). In the other five cases, the dates obtained on hydroxyproline were older than those obtained on collagen at the CIO and ORAU. For these five samples, we suspect that some

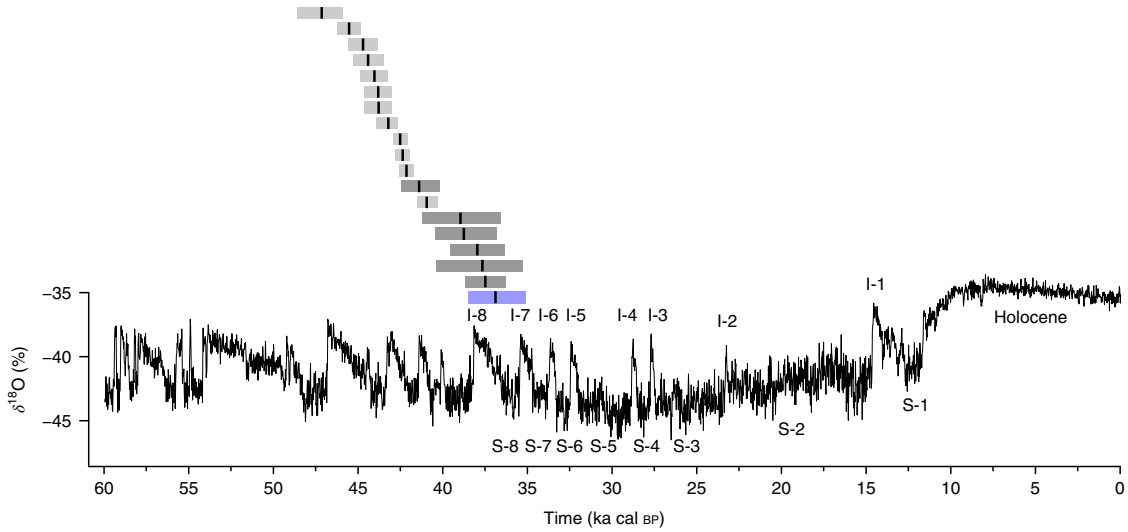

Fig. 3 | Plot of calibrated ages for *E. sibiricum*. Ages were calibrated with IntCal13 in OxCal version 4.3. Median ages are represented as vertical black lines, with 95.4% confidence limits as associated grey bars. HYP dates are shown in darker grey. The blue bar represents our estimate (95.4% posterior distribution) for the last appearance of *Elasmotherium*, as derived from our phase model. The North Greenland Ice Core Project δ^{18}O record is shown as a proxy for temperature (more positive values represent warmer temperatures). The maximum counting error reported for the Greenland time scale (Greenland Ice Core Chronology 2005) is considered to approximate the 2σ uncertainty[80]; for the start of S5 (S-5.1), this is 1,008 years[29]. Greenland stadials (S1 to S8) and interstadials (I1 to I8) are indicated.

contaminant had remained in the collagen (possibly cross-linked to it), but was removed by hydrolysing the collagen and isolating hydroxyproline. Similar observations have been made on a range of contaminated Palaeolithic bone samples (see, for example, refs [12–16]). Ages obtained on hydroxyproline were therefore retained over those obtained from bulk collagen on these nine samples. In the final dataset of conventional radiocarbon ages, 19 are finite dates and 4 are beyond the radiocarbon limit. The five youngest ages were all corroborated by HYP. The 19 finite dates were then calibrated against the IntCal13 dataset[17] using OxCal version 4.3 (ref. [18]) (Supplementary Fig. 2) and incorporated within a single Phase model in OxCal version 4.3 (Supplementary Table 9). We used a general outlier model (with prior probability set at 0.05)[19] to explore the degree to which likelihoods were outlying. Using IntCal13, the calibrated 95.4% confidence intervals for the finite ages range in an overlapping series from 50–44.76 to 38.97–36.52 ka cal BP (Fig. 3 and Supplementary Fig. 2). The end boundary in the model provides an estimate of the last appearance of *Elasmotherium* at 38.48–35.06 ka cal BP (at 95.4% probability). Our data demonstrate the late Quaternary extinction of *E. sibiricum*, and imply an extinction before the Last Glacial Maximum (LGM). With 23 dates, this conclusion is provisional, but it is supported by the lack of any known remains in dated post-LGM contexts[20,21].

Six bone samples were subjected to ancient DNA analysis and all yielded usable DNA data, although molecular preservation varied markedly (Supplementary Table 2). We were able to reconstruct a high-quality mitochondrial genome sequence for the best-preserved specimen—IPAE 915/2804 (GenBank accession: MH937513)—with a mean read depth of 116.1×, which covered 99.3% of the modern white rhinoceros reference (*Ceratotherium simum*; NC_001808). It is notable that IPAE 915/2804, from Tobolsk (latitude ~58° N), is the most northerly of our samples (Fig. 2), possibly accounting for its better DNA preservation. Despite poorer preservation in the other samples—as low as 0.8× depth for 2388/1—all sequences were very similar to IPAE 915/2804 (≥99.7% identical at unambiguously called nucleotide sites).

Phylogenetic analyses including the IPAE 915/2804 consensus sequence strongly suggest that *Elasmotherium* is a sister taxon to Rhinocerotinae (Fig. 4; maximum likelihood bootstrap = 99%; Bayesian posterior probability = 1.0). Relationships among perissodactyls were otherwise concordant with the results of past molecular studies[22,23], although the position of the root of Rhinocerotinae remains poorly resolved.

Our molecular dating analyses suggest that the divergence between *Elasmotherium* and the Rhinocerotinae occurred around 47.3 Ma (95% highest posterior density (HPD) = 41.9–53.2 Ma). The primary divergence within crown Rhinocerotinae (the split between *Diceros* + *Ceratotherium* and the remaining taxa) occurred 30.8 Ma (95% HPD = 26.5–35.3 Ma), while the divergence of Rhinocerotoidea from Tapiroidea occurred 57.5 Ma (95% HPD = 52.6–62.8 Ma). HPDs for node ages estimated in the present study overlapped with those of comparable nodes in previously published studies[23,24]. However, our mean age estimates for nodes deeper in the tree (that is, crown ages of Perissodactyla and Ceratomorpha) were slightly older than those in previously published studies, as our conservative node age constraints allowed for the possibility that perissodactyl diversification began during the Palaeocene (see Supplementary Information).

For stable isotope analysis, carbon-to-nitrogen ratios of all samples were within the acceptable range (Supplementary Table 6), with the exception of sample IPAE 420-111, which was just outside the range and is excluded from further discussion. The *Elasmotherium* δ^{13}C values ($n = 22$) ranged from −21.5 to −16.3‰ with a mean of −18.1 ± 0.3‰. The δ^{15}N values ($n = 21$) ranged from +6.5 to +12.8‰ with a mean of +9.4 ± 0.3‰ (Fig. 5 and Supplementary Table 6). The range of stable isotope values might partly be due to geographic or temporal variation, although no trend through time or correlation with latitude was observed in the data (Supplementary Fig. 1). The *Elasmotherium* δ^{13}C and δ^{15}N values clearly differed from those of other fossil Rhinocerotidae from Eurasia (Fig. 5). The majority of *E. sibiricum* individuals were relatively higher in both δ^{13}C and δ^{15}N than narrow-nosed and/or Merck's rhinoceroses (*Stephanorhinus hemitoechus* and *Stephanorhinus kirchbergensis*, respectively) from the middle Pleistocene of Schöningen, Germany. Most of our samples were also enriched in both δ^{13}C and δ^{15}N compared with the woolly rhinoceros (*C. antiquitatis*) from within the temporal and

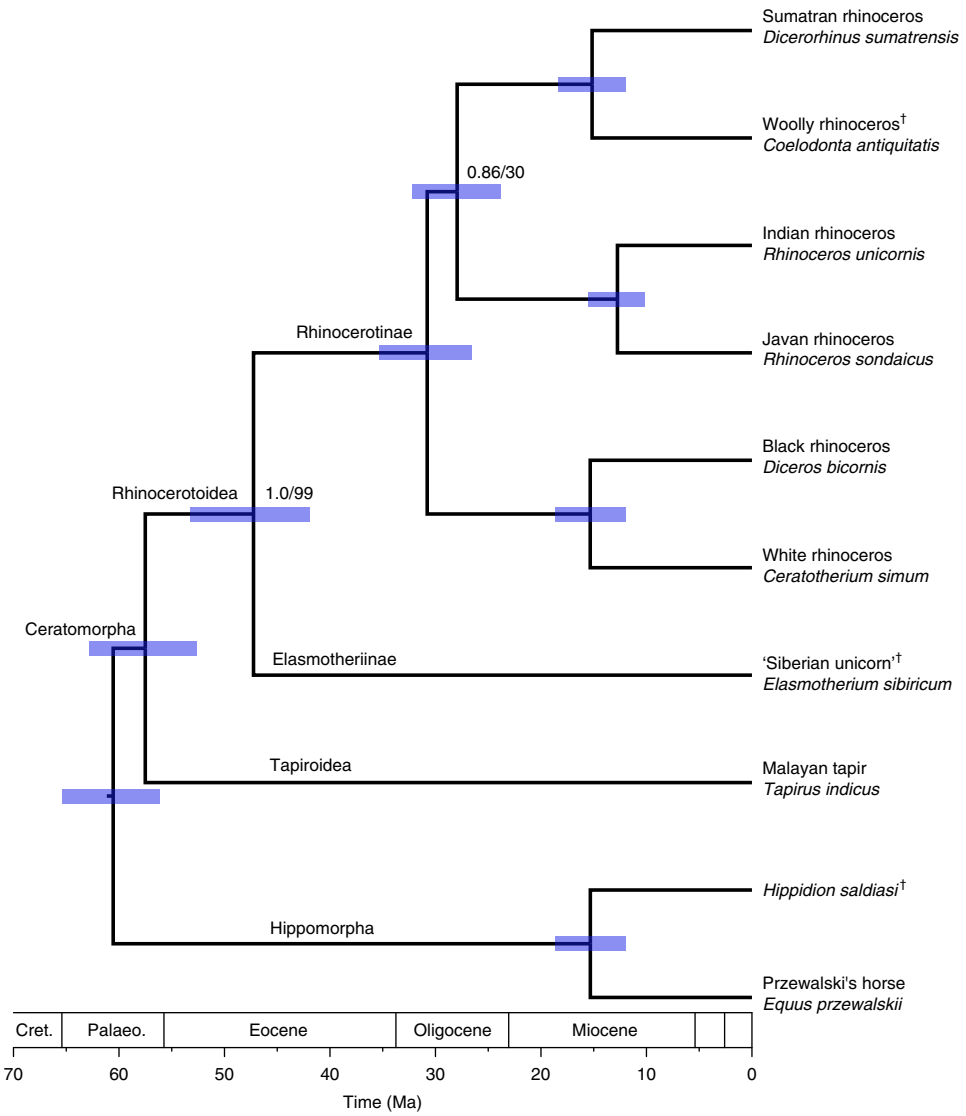

Fig. 4 | Maximum clade credibility tree of rhinoceroses and selected outgroup perissodactyls resulting from our time-calibrated BEAST analyses. Dagger symbols indicate extinct species. Node heights represent mean age estimates, while node bars represent 95% HPDs. Branch support values (BEAST posterior probability/maximum likelihood bootstrap percentage) are presented in black text for nodes that received less than unequivocal support (that is, 1.0/100). Cret., Cretaceous; Palaeo., Palaeocene.

geographical range of the *Elasmotherium* material. Conversely, *E. sibiricum* overlapped strongly with a sample of saiga antelope (*Saiga tatarica*) from the same spatiotemporal range (Fig. 5).

Discussion

Our results have implications for both the phylogenetic position and extinction of the last elasmotheriine rhinoceros, and for the pattern and causality of late Quaternary megafaunal turnover. The deep division between *E. sibiricum* and the extant rhinoceroses in our molecular phylogeny (Fig. 4) is strongly supportive of an ancient split between Elasmotheriinae (including *Elasmotherium*, contra refs [4,5]) and Rhinocerotinae, in keeping with recent palaeontological evidence: the earliest fossil species referred to Elasmotheriinae are *Subhyracodon occidentalis* and *Penetrigonias dakotensis* at around 38 Ma[3,25], while the earliest certain representative of Rhinocerotinae is *Epiaceratherium naduongense*[26] at around 39–35 Ma. Our early- to mid-Eocene estimate of ~47.4 Ma for the divergence between Elasmotheriinae and Rhinocerotinae pre-dates their first fossil appearances by 8–9 Ma, with this lag probably explained by the incompleteness of taxonomic samples included in morphology-based phylogenetic analyses of Rhinocerotidae, especially regarding stem Eocene taxa[2,3].

Previously, the loss of *E. sibiricum* has been regarded as part of the 'background extinction' of large mammals that proceeded through the early and middle Pleistocene. The species was considered typical of the Singhil and Khazar faunistic complexes of Russia, broadly early and late middle Pleistocene, respectively, with its youngest occurrences attributed to the late middle Pleistocene, around 200 ka[7,8]. However, most of the remains, from locations in the Volga region, were found on river banks, with probable mixing of bones from different geological horizons. On the basis of locally associated faunas, a possible late Pleistocene age for some of the remains has been suggested (ref. [9] and page 42 of ref. [2]), but aside from Smelovskaya II these specimens were also recovered ex situ and all radiocarbon dates on associated fauna are infinite (Supplementary Information). A radiocarbon measurement of 26,038 ± 356 yr BP (UBA-30522) was obtained from a partial skull of *E. sibiricum* from Kozhamzhar, Kazakhstan[27], but the context otherwise appeared

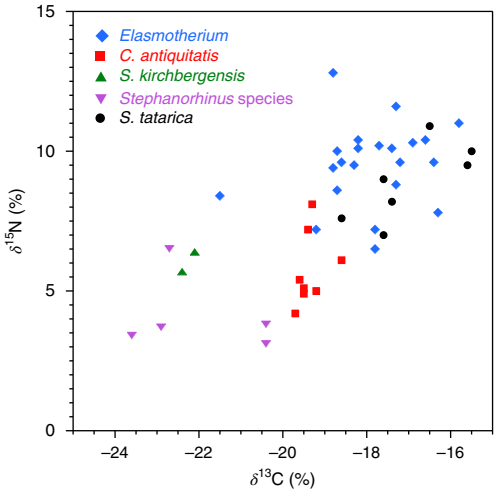

Fig. 5 | Stable carbon (δ^{13}C) and nitrogen (δ^{15}N) values of various species. *E. sibiricum* samples are compared with those of the late Pleistocene woolly rhinoceros (*C. antiquitatis*[37]), middle Pleistocene Merck's rhinoceros (*S. kirchbergensis*[72]), indeterminate middle Pleistocene *Stephanorhinus* specimens (*S. kirchbergensis* or narrow-nosed rhinoceros (*S. hemitoechus*)[73]) and late Pleistocene saiga antelope (*S. tatarica*[54]). *Coelodonta* and *Saiga* data are restricted to the spatiotemporal extent of our *E. sibiricum* samples.

middle Pleistocene, and the laboratory indicated that the date was unreliable as the collagen yield was only 0.3% after ultrafiltration[28].

Our results therefore provide reliably dated late Pleistocene occurrences of *E. sibiricum* ranging from close to the older limit of radiocarbon dating to just before the onset of Greenland stadial 8 (around 36–35 ka; ref. [29]). This places its extinction firmly within the late Quaternary extinction event, during which approximately 40% of northern Eurasian mammal species with bodyweights > 45 kg (megafauna) died out in the interval approximately 50–4 ka[30]. Many of these species became extinct in the late glacial (Greenland interstadial 1 (GI-1) and stadial 1 (S-1)) and Holocene (Marine Isotope Stage 1), starting from around 15 ka. However, the latest dates for *E. sibiricum* around 39–35 ka form an important addition to the growing evidence for turnover in the northern Eurasian large mammal fauna before or early in the LGM[31,32]. The LGM has been variously defined, including the minimum in δ^{18}O in Greenland ice around 30–25 ka (Fig. 3), and the minimum sea level and maximum expansion of Northern Hemisphere ice sheets around 21 ka[33,34]. The latest dates for *E. sibiricum* are closely coincident with those for *Homo neanderthalensis* and the east Beringian stilt-legged horse *Haringtonhippus francisci*[32,35,36]. This was followed by apparent peripheral range reduction in *C. antiquitatis*[32,37], and major genetic turnover in several species including the mammoth and bison[32]. The latest records of Eurasian spotted hyaena *Crocuta crocuta* and cave bear *Ursus spelaeus* are at around 31 ka and 28–27 ka, respectively[38–41], while *Megaloceros giganteus* suffered major range collapse, recovering only in the late glacial (GI-1)[42]. The available dates for *E. sibiricum* strongly corroborate this pre-LGM phase of faunal turnover. There are many fossil localities within the sampled geographical area that have produced later dates for other megafauna[20,37], so the absence of *Elasmotherium* is unlikely to be due to a lack of suitable assemblages.

The inferred timing of these events falls during a period of pronounced climate and environmental change—the series of Greenland stadials and interstadials that characterized Marine Isotope Stage 3 (ref. [32]). The start of this series of dated faunal events, including the last appearance of *E. sibiricum*, is approximately coincident with Greenland stadial 8 and Heinrich stadial 4—a major episode of ice rafting into the North Atlantic[43]. Plant, insect and lithostratigraphic proxies from across northern Eurasia corroborate a sustained shift to cold tundra-steppe beginning around 35 ka BP (equivalent to 40–38 ka), with a breakup of grass/herb-dominated vegetation cover[44]. These changes are a potential contributor to the turnover and extinction of large mammals in the interval preceding the LGM, but further data are required to examine their regional effects in areas such as the central Asian range of *E. sibiricum*.

The extinction of *Elasmotherium* may also have been linked to its high degree of specialization, including extreme dietary adaptations[7]. Among other rhinoceros species, morphological and tooth-wear data show that *S. kirchbergensis* and *S. hemitoechus* were browse- and graze-dominated mixed feeders, respectively, while *C. antiquitatis* was a grazer[45–48]. In *E. sibiricum*, the obtuse angle between the plane of the occiput and the palate indicates that the head was carried even lower than in the woolly rhinoceros and the living white rhinoceros[49,50]—an extreme adaptation to feeding close to the ground. The hypsodont, rootless, permanently growing cheek teeth, with highly convoluted enamel, imply hypergrazing adaptation and/or the consumption of substantial quantities of dust or grit. Our stable isotope analyses of *E. sibiricum* also show values clearly differing from those of other rhinoceros species (Fig. 5). Pollen, plant macrofossil and faunal data suggest that during Marine Isotope Stage 3, the areas inhabited by *E. sibiricum* included open steppe habitats in the southern Trans-Urals, while in other areas forest-steppe landscapes with extensive grassy areas were present[51]. High δ^{13}C and δ^{15}N values, as seen in *E. sibiricum*, are typical for mammals inhabiting a dry steppe or desert biotope[52]. The δ^{13}C values of *E. sibiricum* may also have been influenced by the consumption of Chenopodiaceae (C_4 photosynthesizers), as in the modern saiga antelope *S. tatarica*[53], and/or the pulling up and consumption of roots (as suggested for *E. sibiricum*[7]), since non-photosynthetic plant parts tend to contain elevated δ^{13}C (ref. [54]).

Previous stable isotope studies on mammalian herbivore species from Europe have illustrated change in ecological niches during the pre-LGM[55] and the late glacial[56]. Both *C. antiquitatis* and *S. tatarica* survived the extinction of *E. sibiricum*—*C. antiquitatis* with an isotopic signature implying a dietary niche consistently different from that of *E. sibiricum*, *S. tatarica* with a shift in its range of isotopic values. While *Saiga* samples from pre-LGM central Asia show δ^{13}C and δ^{15}N values overlapping strongly with contemporary *Elasmotherium* (Fig. 5), samples from later periods (LGM to GI-1), and those from other regions, include lower δ^{15}N values (down to +2.8‰), indicating dietary flexibility[53]. The implication is that both *Coelodonta* and *Saiga* could cope with the environmental change that began around 38 ka, but *E. sibiricum* could not. In addition to this, the persistently restricted geographical range of *Elasmotherium* (also probably linked to its specialized habitat), as well as the low population size and slow reproductive rate associated with its large body size[57], would have predisposed it to extinction in the face of environmental change, while the ecologically similar, but much smaller species (*S. tatarica*) survived. The extinction of *E. sibiricum* could in theory have been exacerbated by human hunting pressure, given the replacement of *H. neanderthalensis* by *H. sapiens* in Eurasia around 45–40 ka[58]. There is currently no record of the species' remains from any archaeological site, and the very few suggested depictions of *Elasmotherium* in Palaeolithic art (ref. [50] and pages 46–47 of ref. [2]) are unconvincing.

Methods

We sampled a total of 25 specimens of *E. sibiricum* from the collections of the Museum of the IPAE (Ural Branch of the Russian Academy of Sciences, Ekaterinburg), Sverdlovsk Regional History Museum (Ekaterinburg), Zoological Institute of the Russian Academy of Sciences (Saint Petersburg) and Natural History Museum (London). Specimens were readily identified from the highly characteristic features of the skull, mandible, postcranial bones and hypsodont,

rootless cheek teeth with their distinctive convoluted enamel. Sample provenances are detailed in the Supplementary Information.

At the CIO, samples underwent standard chemical cleaning and collagen extraction following an improved version of the Longin method, as described in ref. [57] and the Supplementary Information. In short, bone samples were decalcified over at least 24 h using weak HCl (4% *w/v*). When CO_2 release had ceased and the fragments were soft and pliable, they were rinsed thoroughly with distilled water. The extract was exposed to NaOH (1%, >30 min) to eliminate humic acids, rinsed to neutrality and again treated with HCl (4% *w/v*, 15 min). The raw collagen fraction was denatured to gelatin in acidified distilled water (pH 3) at 90 °C for 18 h. Dissolved gelatin was filtered through a 100 µm mesh to eliminate any remaining foreign particulates, and dried. The collagen was combusted to CO_2 using an Elemental Analyzer (Isocube) connected to an Isotope Ratio Mass Spectrometer (Isoprime), providing stable isotope ratios for $^{13}C/^{12}C$ and $^{15}N/^{14}N$. For ^{14}C, the CO_2 was cryogenically trapped using an automatic collection device. The routine graphitization procedure at the CIO has been operational for over 20 years[60,61], with only minor, mainly mechanical, adjustments. The $^{14}C/^{12}C$ ratio in the graphite was measured by AMS[62]. At the ORAU, samples were dated using two different methods. First, samples were pretreated following the routine procedure at the ORAU comprising decalcification in acid, a base wash, re-acidification, gelatinization and ultrafiltration (coded 'AF'), as described in ref. [63]. Samples that had been preserved with glues, or samples for which we did not have complete knowledge of post-excavation history, were also washed with organic solvents (acetone, methanol and chloroform) before AF treatment (coded 'AF*'). Samples were also re-dated using the single amino acid radiocarbon dating method optimized at ORAU[11]. This method involves separation of the underivatized amino acids using preparative high performance liquid chromatography after hydrolysis of the bone collagen samples. Using this method, the amino acid hydroxyproline was isolated and then combusted, graphitized and dated by AMS. The sample C/M 12836 was prepared in duplicate as part of an internal control at the ORAU. In both laboratories, the quality of the collagen (or hydroxyproline) extracted was monitored by measuring carbon and nitrogen contents (%C and %N) and the atomic ratio of carbon to nitrogen (C:N) that is acceptable (in the range 2.9–3.5 in the case of collagen or ~5.0 in the case of hydroxyproline).

The ^{14}C ages were calibrated against the Northern Hemisphere calibration (IntCal13) dataset[17]. Here, we used a single 'Phase' model in OxCal 4.3 (ref. [18]) coupled with a 'General' outlier model (probability = 0.05). Using Bayes theorem, the algorithms employed sample possible solutions with a probability that was the product of the prior and likelihood probabilities. Taking into account the deposition model and actual age measurements, the posterior probability densities quantified the most likely age distributions; the 'outlier' option was used to detect ages that fell outside the calibration model for each group and, if necessary, down-weight their contribution to the final age estimates. The 'Phase' command is a grouping model. It assumes no geographic relationship between samples, and that the ages represent a uniform distribution between a start and end boundary. For the model, a start and end boundary were included to bracket the *Elasmotherium* 'phase'. The posterior distributions allowed us to determine probability distribution functions (PDFs) for the beginning and end of the phase. Modelled ages are reported here at the 95% probability range in thousands of calendar years BP (cal ka BP; relative to AD 1950). This method has been applied to a wide range of contexts including studies on megafaunal and Neanderthal extinction[35,64], archaeological phases of occupation and ceramic development[65,66], and palaeoearthquakes[67], providing robust age estimates for the start and end of phases, often with fewer ^{14}C measurements than those reported here. In OxCal, commands or parameters are written in CQL (Contextual Query Language).

The $\delta^{13}C$ and $\delta^{15}N$ values in bone collagen of a herbivorous mammal reflect the isotopic composition of the plant food and water the organism ingested during its life[68], and these are in turn related to climatic and local environmental parameters. The $\delta^{13}C$ and $\delta^{13}N$ values of terrestrial C_3 plants are mainly determined by (local) environmental and biogeochemical factors, such as humidity, atmospheric CO_2 concentrations, nitrogen cycling and nutrient availability[69–71]. The stable carbon and nitrogen isotope concentrations ($\delta^{13}C$ and $\delta^{15}N$ values) of *E. sibiricum* bone collagen were measured on CO_2 by isotope ratio mass spectrometry. Published comparative data comprised the woolly rhinoceros (*C. antiquitatis*)[37], Merck's rhinoceros (*S. kirchbergensis*) and indeterminate *Stephanorhinus* specimens (*S. kirchbergensis* and/or the narrow-nosed rhinoceros *S. hemitoechus*)[72], and saiga antelope (*S. tatarica*)[53]. In the case of *C. antiquitatis* and *S. tatarica*, we plotted only samples from pre-LGM central Asia, for direct comparison with *E. sibiricum*.

Ancient DNA analyses were performed at the Australian Centre for Ancient DNA, University of Adelaide. DNA was extracted from six *E. sibiricum* samples using a silica-based method[73]. Sequencing libraries were then created from the DNA extracts following the protocol of ref. [74]. We enriched each of the sequencing libraries for mammalian mitochondrial DNA using a previously published set of RNA probes[75] and sequenced them on an Illumina MiSeq. The resulting sequencing reads were mapped to the mitochondrial genome of the extant white rhinoceros *C. simum*, and consensus sequences were generated for each sample using Geneious (Biomatters; http://www.geneious.com). Phylogenetic analyses were performed on these data using BEAST (Bayesian Evolutionary Analysis by Sampling Trees)[76] and RAxML (Randomized Axelerated Maximum Likelihood)[77]. Additional details can be found in the Supplementary Information.

Reporting Summary. Further information on research design is available in the Nature Research Reporting Summary linked to this article.

Code availability. The code used to calibrate the ^{14}C ages in OxCal is given in the Supplementary Information.

Data availability

The four mitochondrial genome consensus sequences with coverage ≥80% and mean read depth ≥5× are available on GenBank (MH937513-MH937516). All consensus sequences, unmapped sequencing reads and phylogenetic analysis files associated with our ancient DNA work are available on Figshare (https://doi.org/10.25909/5ba34a40ba925). All the radiocarbon data generated at the ORAU and CIO are archived internally at the respective laboratories, and are available upon request. ORAU data are also available on the laboratory's website, along with a link to the paper.

Received: 27 June 2017; Accepted: 16 October 2018;
Published online: 26 November 2018

References

1. Fortelius, M. *New and Old Worlds Database of Fossil Mammals (NOW)* (Univ. Helsinki, 2017).
2. Antoine, P.-O. Phylogénie et évolution des Elasmotheriina (Mammalia, Rhinocerotidae). *Mém. Mus. Natl Hist.Nat.* **188**, 1–359 (2002).
3. Becker, D., Antoine, P. O. & Maridet, O. A new genus of Rhinocerotidae (Mammalia, Perissodactyla) from the Oligocene of Europe. *J. Syst. Palaeontol.* **11**, 947–972 (2013).
4. Cerdeño, E. Cladistic analysis of the family Rhinocerotidae (Perissodactyla). *Am. Mus. Novit.* **3143**, 1–25 (1995).
5. Guérin, C. & Pickford, M. *Ougandatherium napakense* nov. gen. nov. sp., le plus ancien Rhinocerotidae Iranotheriinae d'Afrique. *Ann. Paléontol.* **89**, 1–35 (2003).
6. Deng, T. & Zheng, M. Limb bones of *Elasmotherium* (Rhinocerotidae, Perissodactyla) from Nihewan (Hebei, China). *Vert. PalAs.* **43**, 110–121 (2005).
7. Schvyreva, A. K. On the importance of the representatives of the genus *Elasmotherium* (Rhinocerotidae, Mammalia) in the biochronology of the Pleistocene of Eastern Europe. *Quat. Int.* **379**, 128–134 (2015).
8. Kozamkulova, B. S. *Elasmotherium sibiricum* und sein Verbreitungsgebiet auf dem Territorium der UdSSR. *Quartärpaläontologie* **4**, 85–91 (1981).
9. Kosintsev, P. A. in *The Quaternary of the Urals: Global Trends and Pan-European Quaternary Records* (eds Borodin, A. V., Markova, E. A. & Strukova, T. V.) 67–68 (UrFU, Ekaterinburg, 2014)..
10. Lister, A. M. & Stuart, A. J. Extinction chronology of the woolly rhinoceros *Coelodonta antiquitatis*: reply to Kuzmin. *Quat. Sci. Rev.* **62**, 144–146 (2013).
11. Devièse, T., Comeskey, D., McCullagh, J., Bronk Ramsey, C. & Higham, T. New protocol for compound-specific radiocarbon analysis of archaeological bones. *Rapid Commun. Mass Spectrom.* **32**, 373–379 (2018).
12. Bourrillon, R. et al. A new Aurignacian engraving from Abri Blanchard, France: implications forunderstanding Aurignacian graphic expression in Western and Central Europe. *Quat. Int.* **491**, 46–64 (2018).
13. Devièse, T. et al. Direct dating of Neanderthal remains from the site of Vindija Cave and implications for themiddle to upper Paleolithic transition. *Proc. Natl Acad. Sci. USA* **114**, 10606–10611 (2017).
14. Reynolds, N., Dinnis, R., Bessudnov, A. A., Devièse, T. & Higham, T. The Kostënki 18 child burial and thecultural and funerary landscape of mid upper Palaeolithic European Russia. *Antiquity* **91**, 1435–1450 (2017).
15. Devièse, T. et al. Increasing accuracy for the radiocarbon dating of sites occupied by the first Americans. *Quat. Sci. Rev.* **198**, 171–180 (2018).
16. Becerra-Valdivia, L. et al. Reassessing the chronology of the archaeological site of Anzick. *Proc. Natl Acad. Sci. USA* **115**, 7000–7003 (2018).
17. Reimer, P. J. et al. Intcal13 and Marine13 radiocarbon age calibration curves 0–50,000 years cal BP. *Radiocarbon* **55**, 1869–1887 (2013).
18. Bronk Ramsey, C. Recent and planned developments of the program OxCal. *Radiocarbon* **55**, 720–730 (2013).
19. Bronk Ramsey, C. Bayesian analysis of radiocarbon dates. *Radiocarbon* **51**, 337–360 (2009).
20. Kosintsev, P. A. *Ural and Siberia Faunas at Pleistocene and Holocene Times* (IPAE UB RAS, Chelyabinsk, 2005).
21. Vasil'ev, S. A. Faunal exploitation, subsistence practices and Pleistocene extinctions in Palaeolithic Siberia. *Deinsea* **9**, 513–556 (2003).
22. Price, S. A. & Bininda-Emonds, O. R. P. A comprehensive phylogeny of extant horses, rhinos and tapirs (Perissodactyla) through data combination. *Zoosystematics Evol.* **85**, 277–292 (2009).

23. Steiner, C. C. & Ryder, O. A. Molecular phylogeny and evolution of the Perissodactyla. *Zool. J. Linn. Soc.* **163**, 1289–1303 (2011).
24. Meredith, R. W. et al. Impacts of the Cretaceous terrestrial revolution and KPg extinction on mammal diversification. *Science* **334**, 521–524 (2011).
25. Heissig, K. The American genus *Penetrigonias* Tanner & Martin, 1976 (Mammalia: Rhinocerotidae) as a stem group elasmothere and ancestor of *Menoceras* Troxell, 1921. *Zitteliana* **A 52**, 79–95 (2012).
26. Boehme, M. et al. Na Duong (northern Vietnam)—an exceptional window into Eocene ecosystems from Southeast Asia. *Zitteliana* **A 53**, 120–167 (2013).
27. Shpansky, A. V., Ilyina, S. A. & Aliyasova, V. N. The Quaternary mammals from Kozhamzhar locality (Pavlodar Region, Kazakhstan). *Am. J. Appl. Sci.* **13**, 189–199 (2016).
28. Reimer, P. J. & Svyatko, S. V. Comment on Shpansky et al. 2016, The Quaternary mammals fromKozhamzhar locality (Pavlodar region, Kazakhstan). *Am. J. Appl. Sci.* **13**, 477–478 (2016).
29. Rasmussen, S. O. et al. A stratigraphic framework for abrupt climatic changes during the Last Glacial period based on three synchronized Greenland ice-core records: refining and extending the INTIMATE event stratigraphy. *Quat. Sci. Rev.* **106**, 14–28 (2014).
30. Stuart, A. J. Late Quaternary megafaunal extinctions on the continents: a short review. *Geol. J.* **50**, 338–363 (2015).
31. Stuart, A. J. & Lister, A. M . Patterns of late Quaternary megafaunal extinctions in Europe and northern Asia. *Cour. Forsch. Inst. Senckenberg* **259**, 289–299 (2007).
32. Cooper, A. Abrupt warming events drove Late Pleistocene Holarctic megafaunal turnover. *Science* **349**, 602–606 (2015).
33. Hughes, P. D. & Gibbard, P. L. A stratigraphical basis for the Last Glacial Maximum (LGM). *Quat. Int.* **383**, 174–185 (2015).
34. Monegato, G., Scardia, G., Hajdas, I., Rizzini, F. & Piccin, A. The Alpine LGM in the boreal ice-sheets game. *Sci. Rep.* **7**, 2078 (2017).
35. Higham, T. et al. The timing and spatiotemporal patterning of Neanderthal disappearance. *Nature* **512**, 306–309 (2014).
36. Heintzman, P. D. et al. A new genus of horse from Pleistocene North America. *eLife* 6, e29944 (2017)..
37. Stuart, A. J. & Lister, A. M. Extinction chronology of the woolly rhinoceros *Coelodonta antiquitatis* in the context of late Quaternary megafaunal extinctions in northern Eurasia. *Quat. Sci. Rev.* **51**, 1–17 (2012).
38. Stuart, A. J. & Lister, A. M. New radiocarbon evidence on the extirpation of the spotted hyaena (*Crocuta crocuta* (Erxl.)) in northern Eurasia. *Quat. Sci. Rev.* **96**, 108–116 (2014).
39. Dinnis, R., Pate, A. & Reynolds, N. Mid-to-late Marine Isotope Stage 3 mammal faunas of Britain: a new look. *Proc. Geol. Assoc.* **127**, 435–444 (2016).
40. Pacher, M. & Stuart, A. J. Extinction chronology and palaeobiology of the cave bear (*Ursus spelaeus*). *Boreas* **38**, 189–206 (2009).
41. Bocherens, H. et al. The last of its kind? Radiocarbon, ancient DNA and stable isotope evidence from a late cave bear (*Ursus spelaeus* ROSENMÜLLER, 1794) from Rochedane (France). *Quat. Int.* **339–340**, 179–188 (2014).
42. Stuart, A. J., Kosintsev, P. A., Higham, T. & Lister, A. M. Pleistocene to Holocene extinction dynamics in giant deer and woolly mammoth. *Nature* **431**, 684–689 (2004).
43. Guillevic, M. et al. Evidence for a three-phase sequence during Heinrich stadial 4 using a multiproxy approach based on Greenland ice core records. *Clim. Past* **10**, 2115–2133 (2014).
44. Hubberten, H. W. et al. The periglacial climate and environment in northern Eurasia during the Last Glaciation. *Quat. Sci. Rev.* **23**, 1333–1357 (2004).
45. Boeskorov, G. G. et al. Woolly rhino discovery in the lower Kolyma River. *Quat. Sci. Rev.* **30**, 2262–2272 (2011).
46. Rivals, F. & Lister, A. M. Dietary flexibility and niche partitioning of large herbivores through the Pleistocene of Britain. *Quat. Sci. Rev.* **146**, 116–133 (2016).
47. Saarinen, J., Eronen, J., Fortelius, M., Seppä, H. & Lister, A. M. Patterns of diet and body mass of large ungulates from the Pleistocene of Western Europe, and their relation to vegetation. *Palaeontol. Electron.* **19**, 1–58 (2016).
48. Pushkina, D., Bocherens, H. & Ziegler, R. Unexpected palaeoecological features of the middle and latePleistocene large herbivores in southwestern Germany revealed by stable isotopic abundances in tooth enamel. *Quat. Int.* **339-340**, 164–178 (2014).
49. Zeuner, F. E. New reconstructions of the woolly rhinoceros and Merck's rhinoceros. *Proc. Linn. Soc. Lond.* **156**, 183–195 (1945).
50. Zhegallo, V. et al. On the fossil rhinoceros *Elasmotherium* (including the collections of the Russian Academy of Sciences). *Cranium* **22**, 17–40 (2005).
51. Grichuk, V. P. *Dynamics of Terrestrial Landscape Components and Inner Marine Basins of Northern Eurasia During the Last 130,000 Years* (ed. Velichko, A. A.) 64–88 (GEOS, Moscow, 2002).
52. Bocherens, H. Isotopic biogeochemistry and the paleoecology of the mammoth steppe fauna. *Deinsea* **9**, 57–76 (2003).
53. Jürgensen, J. et al. Diet and habitat of the saiga antelope during the late Quaternary using stable carbon and nitrogen isotope ratios. *Quat. Sci. Rev.* **160**, 150–161 (2017).
54. Badeck, F.-W., Tcherkez, G., Nogués, S., Piel, C. & Ghashghaie, J. Post-photosynthetic fractionation of stable carbon isotopes between plant organs—a widespread phenomenon. *Rapid Commun. Mass Spectrom.* **19**, 1381–1391 (2005).
55. Drucker, G. et al. Tracking possible decline of woolly mammoth during the Gravettian in Dordogne (France) and the Ach Valley (Germany) using multi-isotope tracking (^{13}C, ^{14}C, ^{15}N, ^{34}S, ^{18}O). *Quat. Int.* **360**, 304–317 (2015).
56. Drucker, D. G., Bocherens, H. & Péan, S. Isotopes stables (^{13}C, ^{15}N) du collagène des mammouths de Mezhyrich (Epigravettien, Ukraine): implications paléoécologiques. *L'Anthropologie* **118**, 504–517 (2014).
57. Johnson, C.N. Determinants of loss of mammal species during the late Quaternary 'megafauna' extinctions: life history and ecology, but not body size. *Proc. R. Soc. B* **269**, 2221–2227 (2009)..
58. Higham, T. et al. The timing and spatiotemporal patterning of Neanderthal disappearance. *Nature* **512**, 306–309 (2014).
59. Mook, W. G. & Streurman, H. J. Physical and chemical aspects of radiocarbon dating. In *Proc. 1st Symposium on C and Archaeology* (eds Mook, W. G. & Waterbolk, H. T.) 31–55 (PACT, Groningen, 1983).
60. Wijma, S., Aerts, A. T., van der Plicht, J. & Zondervan, A. The Groningen AMS facility. *Nucl. Instrum. Methods Phys. Res. B* **113**, 465–469 (1996).
61. Aerts-Bijma, A. T., Meijer, H. A. J. & van der Plicht, J. AMS sample handling in Groningen. *Nucl. Instrum. Methods Phys. Res. B* **123**, 221–225 (1997).
62. Van der Plicht, J., Wijma, S., Aerts, A. T., Pertuisot, M. H. & Meijer, H. A. J. Status report: the Groningen AMS facility. *Nucl. Instrum. Methods Phys. Res. B* **172**, 58–65 (2000).
63. Brock, F., Higham, T., Ditchfield, P. & Ramsey, C. B. Current pretreatment methods for AMS radiocarbon dating at the Oxford Radiocarbon Accelerator Unit (ORAU). *Radiocarbon* **52**, 103–112 (2010).
64. Metcalf, J. L. et al. Synergistic roles of climate warming and human occupation in Patagonian megafaunal extinctions during the Last Deglaciation. *Sci. Adv.* **2**, e1501682 (2016).
65. Turney, C. S. M., Jones, R. T., Thomas, Z. A., Palmer, J. G. & Brown, D. Extreme wet conditions coincident with Bronze Age abandonment of upland areas in Britain. *Anthropocene* **13**, 69–79 (2016).
66. Finkelstein, I. & Piasetzky, E. Radiocarbon dating the Iron Age in the Levant: a Bayesian model for six ceramic phases and six transitions. *Antiquity* **84**, 374–385 (2010).
67. Lienkaemper, J. J. & Ramsey, C. B. OxCal: versatile tool for developing paleoearthquake chronologies—a primer. *Seismol. Res. Lett.* **80**, 431–434 (2009).
68. Kohn, M. J. You are what you eat. *Science* **283**, 335–336 (1999).
69. Szpak, P. Complexities of nitrogen isotope biogeochemistry in plant–soil systems: implications for the study of ancient agricultural and animal management practices. *Front. Plant Sci.* **5**, 288 (2014).
70. Nadelhoffer, K. et al. ^{15}N natural abundances and N use by tundra plants. *Oecologia* **107**, 386–394 (1996).
71. Michener, R. & Lajtha, K. *Stable Isotopes in Ecology and Environmental Science* (Blackwell, Oxford, 2007).
72. Kuitems, M. et al. Carbon and nitrogen stable isotopes of well-preserved, middle Pleistocene bone collagenfrom Schöningen (Germany) and their palaeoecological implications. *J. Hum. Evol.* **89**, 105–113 (2015).
73. Brotherton, P. et al. Neolithic mitochondrial haplogroup H genomes and the genetic origins of Europeans. *Nat. Commun.* **4**, 1764 (2013).
74. Meyer, M. & Kircher, M. Illumina sequencing library preparation for highly multiplexed target capture and sequencing. *Cold Spring Harb. Protoc.* **5**, pdb.prot5448 (2010).
75. Mitchell, K. J. et al. Ancient mitochondrial DNA reveals convergent evolution of giant short-faced bears (Tremarctinae) in North and South America. *Biol. Lett.* **12**, 20160062 (2016).
76. Drummond, A. J. & Rambaut, A. BEAST: Bayesian evolutionary analysis by sampling trees. *BMC Evol. Biol.* **7**, 214 (2007).
77. Stamatakis, A. RAxML version 8: a tool for phylogenetic analysis and post-analysis of large phylogenies. *Bioinformatics* **30**, 1312–1313 (2014).
78. Rohling, E. J. et al. New constraints on the timing of sea level fluctuations during early to middle MarineIsotope Stage 3. *Paleoceanography* **23**, PA3219 (2008).
79. Ehlers, J. & Gibbard, P. L. *Quaternary Glaciations: Extent and Chronology* Parts 1-3 (Developments inQuaternary Science 2, Elsevier, Amsterdam, 2004).
80. Andersen, K. K. et al. The Greenland ice core chronology 2005, 15–42 ka. Part 1: constructing the time scale. *Quat. Sci. Rev.* **25**, 3246–3257 (2006).

Acknowledgements

We thank P.-O. Antoine for discussion, J. Saarinen for estimating the body mass of *Elasmotherium*, the Museum of the IPAE UB RAS and L. Petrov for providing bone samples for analysis, P. Campos for help with the stable isotope data, S. Brace for initial work on ancient DNA, the team of the ORAU for AMS dating and J. Hagstrum for an early stimulus to the study. Funding was provided by the Australian Research Council and Natural Environment Research Council, UK (grant number NE/G005982/1). Funding for part of the research was provided by the European Research Council under

the European Union's Seventh Framework Programme (FP7/2007-2013)—ERC grant 324139 'PalaeoChron' award to T.H. This study was partly supported by the programme of the UB RAS (project number 18-4-4-3).

Author contributions

P.K., T.v.K., A.J.S., A.M.L. and A.C. conceived the project. P.K., A.T. and E.P. provided samples and contextual information. Ancient DNA work and phylogenetic analyses were performed by K.J.M. and coordinated by A.C. Radiocarbon data were obtained and analysed by T.H., T.D. and D.C. at the ORAU, and J.v.d.P. at the CIO, while C.T. and T.H. undertook age modelling. Stable isotope analysis was performed and interpreted by M.K., while C.T. and A.J.S. provided context on climate and extinctions, respectively. All authors contributed to interpretation of the results and writing of the manuscript, which was coordinated by A.M.L.

Competing interests

The authors declare no competing interests.

Additional information

Supplementary information is available for this paper at https://doi.org/10.1038/s41559-018-0722-0.

Reprints and permissions information is available at www.nature.com/reprints.

Correspondence and requests for materials should be addressed to A.M.L.

Publisher's note: Springer Nature remains neutral with regard to jurisdictional claims in published maps and institutional affiliations.

© The Author(s), under exclusive licence to Springer Nature Limited 2018